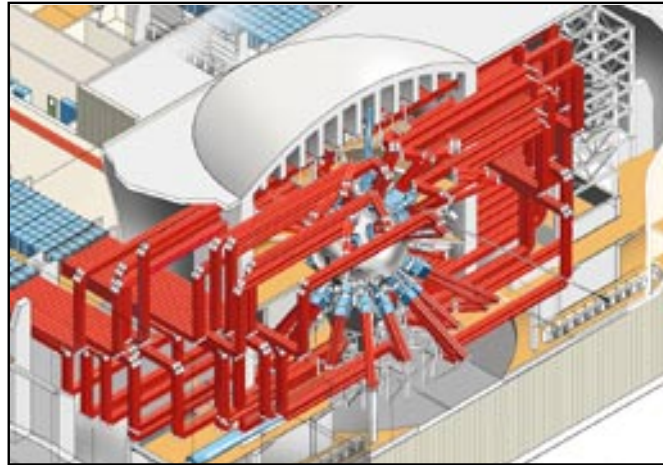


# A Tour of the Proposed National Ignition Facility



*On a conceptual walk-through of the proposed National Ignition Facility, we follow the path of a photon from the master oscillator and preamplifier at the beginning of the laser chain, through the main laser components, to the target. We conclude with the results of our recent Beamlet Demonstration Project, which demonstrated a prototype of one of the 192 laser beams that will be required to achieve ignition and energy gain in inertial confinement fusion targets.*

**T**HE National Ignition Facility (NIF) will house the world's most powerful laser system. **Figure 1** is an artist's sketch of the proposed laser and target area building. The overall floor plan is U shaped, with laser bays forming the legs of the U, and switchyards and the target area forming the connection.

The NIF will contain 192 independent laser beams, each of which is called a "beamlet." Each beamlet will have a square aperture of a little less than 40 centimeters on a side. Beamlets are grouped mechanically into four large arrays—or bundles of beamlines—with the beamlets stacked four high and twelve wide, as shown in blue on the left-hand side of the sketch. The 192

laser beamlines require more than 9000 discrete, large optics (larger than  $40 \times 40$  cm) and several thousand additional smaller optics.

The laser output beams strike a series of mirrors, which redirect them to the large target chamber shown on the right side of **Figure 1**. From switchyards to the target chamber room, the beams are in groups of four ( $2 \times 2$  arrays) and follow the beam paths shown in red. At the target chamber, the beams pass through frequency-conversion crystals that convert the infrared laser output beams to ultraviolet laser light. They then pass through lenses that focus the ultraviolet beams on a tiny target located in the center of the target chamber.

To give some perspective on its overall dimensions, the NIF building is roughly 200 meters long  $\times$  85 meters wide (about  $600 \times 250$  feet). These dimensions are a little smaller than those of a typical covered football stadium. As an example, **Figure 2** compares the NIF building with the Minneapolis Metrodome.

This article takes us on a tour of the proposed facility. First, we follow the complex path of a photon from the master oscillator at the beginning of the laser chain, through the laser components, and on to the target. After this tour, we discuss some of the principal laser components and target experiments in more detail. Finally, we describe the results of the Beamlet Demonstration Project that

was recently completed at LLNL. As part of its core activities, the Inertial Confinement Fusion (ICF) Program developed a prototype of a single beamlet of NIF to validate the technology needed for the next generation of glass-laser drivers.

### Master Oscillator

We begin our tour approximately in the center of the facility, where a laser pulse is born in the master oscillator room. Here, four oscillators made of neodymium-doped optical

fiber generate weak laser pulses at four separate frequencies (or colors of light). Each pulse is launched into an optical fiber system that amplifies and splits the pulse into 192 separate fibers, 48 of each color. The four colors are used to smooth the intensity (power per unit area) of the laser spot on the target.

The optical fibers carry the laser pulses to 192 low-voltage optical modulators. The modulators for NIF were derived from the integrated-optics modulators that are now being installed in very-high-speed optical

fiber communications networks. The modulators allow us to tailor the pulse shape independently in each beamlet under computer control. In this way, the 192 pulses can be carefully shaped and balanced to set up exactly the conditions an experimenter needs on a target without rearranging any laser hardware in the facility. An optical fiber then carries the individually tailored pulse to each beamlet. The power in the laser pulse at this point is a little less than a watt. Typical pulses are a few nanoseconds long

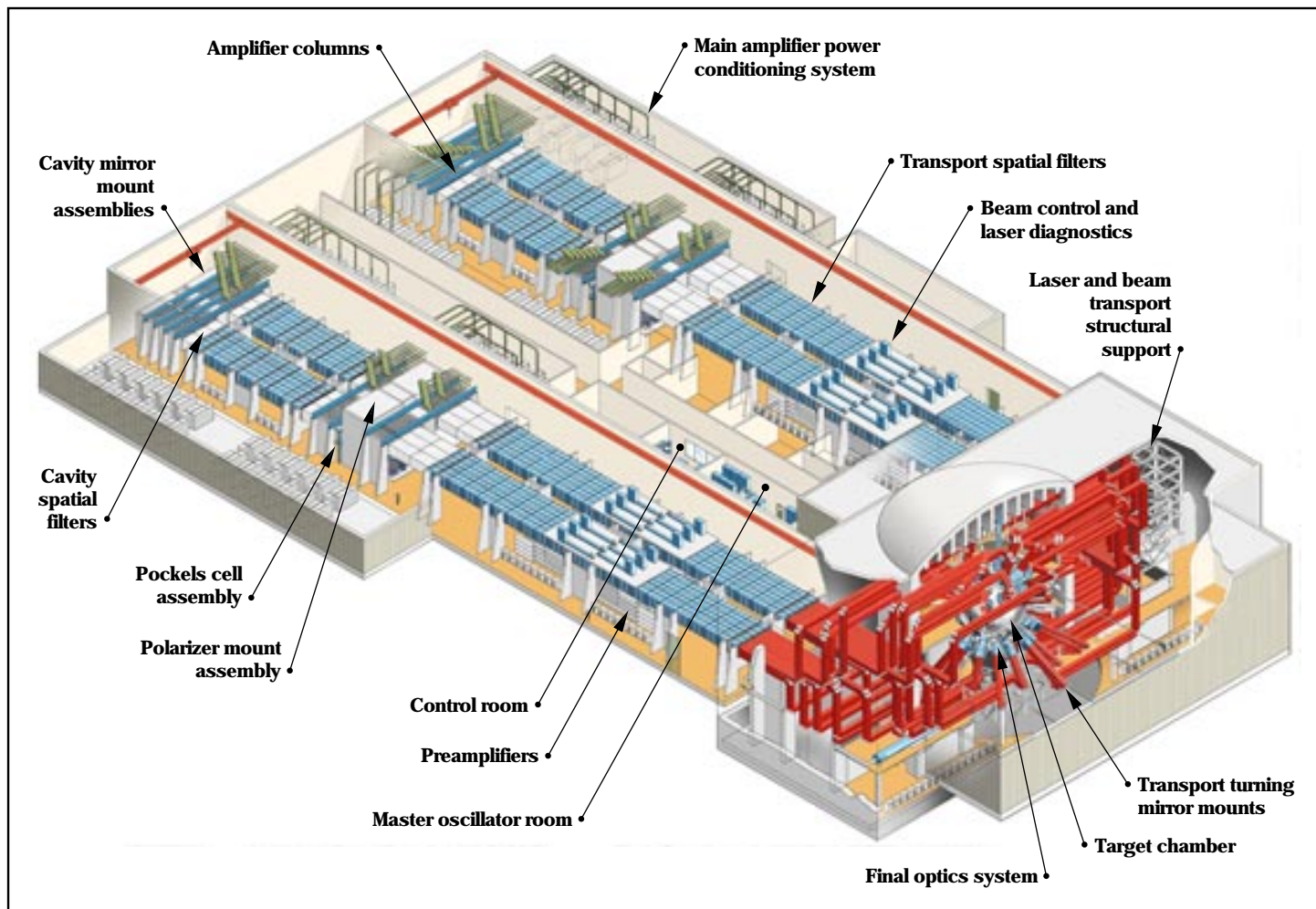


**Figure 1.** View of the proposed laser and target area building for NIF. This facility will contain the world's most powerful neodymium glass laser system, 50 times more powerful than Nova, currently the world's most powerful laser. This sketch shows the laser bays, which form the two legs of the U-shaped floor plan, and the switchyards and target area forming the connection.

(a nanosecond is  $10^{-9}$  second), so the energy is a few nanojoules (a nanojoule is  $10^{-9}$  joule).

### Preamplifier

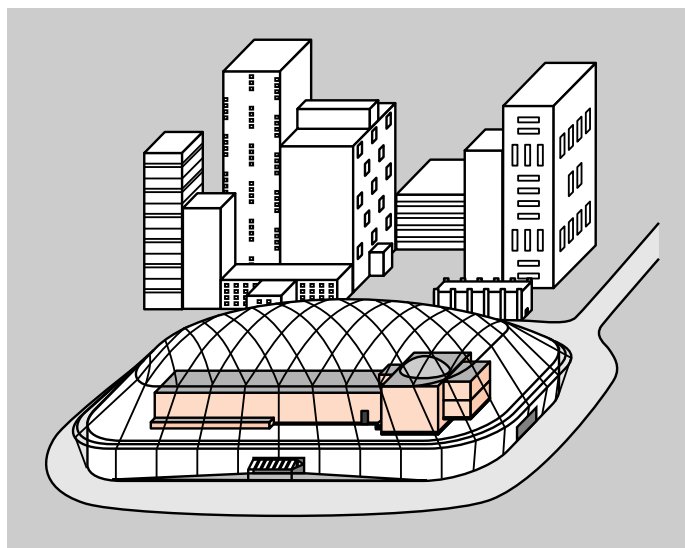
Optical fibers carrying the pulses from the master oscillator room spread out to 192 preamplifier packages. As shown in Figure 1, the NIF preamplifiers are located beneath the focal plane at the center of the large transport spatial filters, which are located between the laser components and the target chamber.

Each preamplifier package has a regenerative amplifier in a ring cavity. This device amplifies the pulse by a factor of about a million, from about a nanojoule to a millijoule, with very high stability. The amplifier uses small neodymium glass amplifiers pumped by semiconductor laser diodes so that it has very stable gain and requires little servicing. The laser pulse then enters spatial beam-shaping optics and a flashlamp-pumped, four-pass rod amplifier, which converts it to about a 1-J pulse with the spatial intensity profile needed for injection into the main laser cavity.

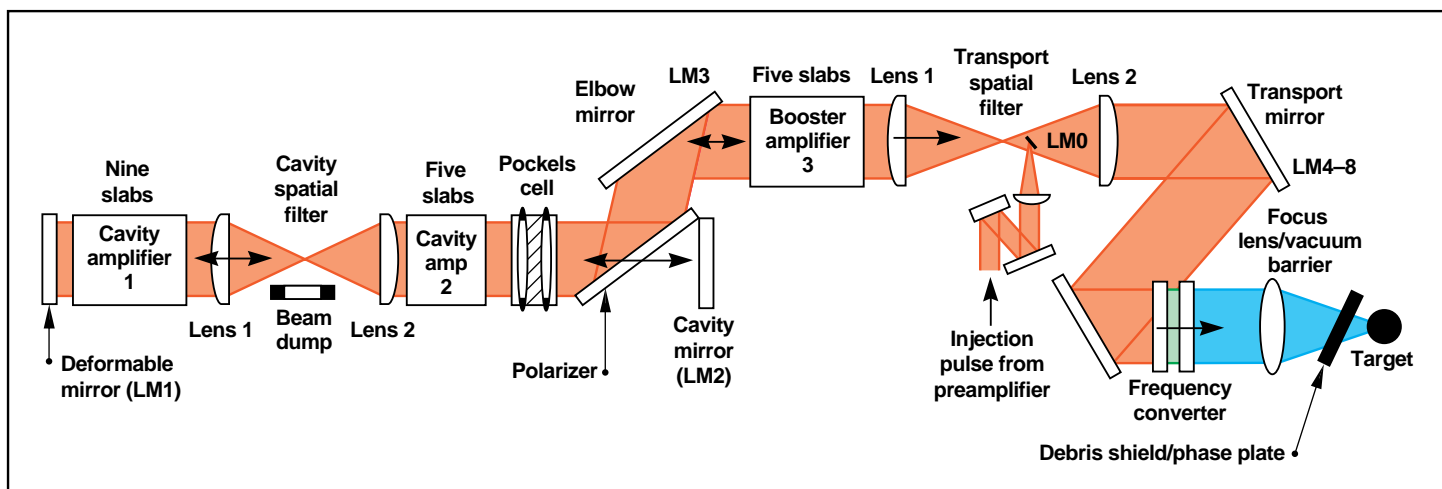
### Following a Pulse Through the Main Laser Components

Figure 3 shows the layout of the main laser components of a NIF beamlet. These components take the laser pulse from the preamplifier all the way to a frequency-converted pulse headed to the target. We first follow a pulse through the various components and then discuss their functions in more detail.

A pulse of laser light from the preamplifier reflects from a small mirror labeled LM0 in Figure 3. This mirror is located near the focal plane of the pair of lenses labeled lens 1 and 2 and identified as the transport spatial filter. Light comes to a focus at the focal plane of the transport spatial filter and re-expands to a size of a little less than 40 cm at lens 1 of the spatial filter, where it again becomes a parallel beam. The beam



**Figure 2.** The NIF building is similar in size to a modern municipal stadium. For perspective, the NIF building is compared here to the Minneapolis Metrodome.



**Figure 3.** One beamlet of the NIF laser, from pulse injection to final focus on the target. We designed the laser chain in this beamline using the CHAINOP family of numerical codes. These codes model the performance and cost of high-power, solid-state inertial confinement fusion laser systems. The path taken by a photon is described in the text.

passes through booster amplifier 3, reflects from the polarizer, is amplified further in cavity amplifier 2, and goes through a second spatial filter identified as the cavity spatial filter. After passing through amplifier 1, the beam reflects from a deformable mirror (mirror LM1 at the far left end of Figure 3). After once again passing through amplifier 1, the beam comes back through the cavity spatial filter and amplifier 2.

Meanwhile, the component identified as the Pockels cell in Figure 3 is energized. This important component rotates the plane of polarization of the laser light from horizontal to vertical. In this polarization, the pulse passes through the polarizer and strikes mirror LM2, which redirects it back once again towards mirror LM1. The Pockels cell rotates the polarization back to horizontal, and the beam passes back through amplifier 2 and the cavity spatial filter and makes another double pass through amplifier 1, reflecting from LM1. It then passes through the cavity spatial filter and amplifier 2 one more time.

By this time, the Pockels cell has been de-energized so that it no longer rotates the polarization of the pulse. As a consequence, the pulse reflects from the polarizer and is further

amplified by amplifier 3 to an energy of about 17 kJ for a typical ignition target pulse shape. Now the pulse passes through the transport spatial filter on a path slightly displaced from the input path. Because it is displaced, the output pulse just misses the injection mirror LM0, the mirror where laser light was first reflected when it came from the preamplifier.

The pulse travels through a long beam path reflecting from several transport mirrors until it reaches the target chamber. (For simplicity, Figure 3 does not show all the transport mirrors that will be installed in NIF.) Mounted on the target chamber is a frequency converter that changes the infrared laser pulse to ultraviolet laser light. A focusing lens brings the ultraviolet pulse to a focus at the center of the target chamber. A debris shield protects the focusing lens from any target fragments and may also have a pattern etched into its surface to reshape the distribution of laser intensity in the focal spot on the target.

Four pulses from different beamlets, each at a slightly different color or frequency, come to a focus at a single spot on the target. The intensity profile of the sum of these four spots is much smoother than the

profile of each spot individually. Smooth intensity profiles lead to better-understood experimental conditions and better target performance.

An important feature of NIF is its integrated computer control system. This system uses a high-speed optical fiber network to connect roughly 25,000 control points, sensors, and distributed processors. The items that are controlled by computer include motors and switches for alignment, diagnostic systems for the laser beams, data from target diagnostics, data processing stations, and all other control and information features of the facility.

## More About the Main Laser Components

### Amplifiers

Figure 4 is a top-down view of a glass amplifier. The NIF amplifiers are constructed from slabs of neodymium-doped phosphate glass set vertically on edge at Brewster's angle to the beam. At this angle, horizontally polarized beams have very low reflective losses while propagating through the plates. The glass slabs are  $46 \times 81$  cm to give a clear aperture of  $40 \times 40$  cm from the beam's point of view.

Figure 5 shows how the amplifier slabs are grouped together into large arrays. Such grouping reduces the number of required parts and floor space, hence the cost of the facility. Long xenon flashlamps extend vertically across a stack of four slabs, an arrangement resulting in a length that is convenient for the pulsed-power system that drives the flashlamps. The width of 12 slabs is convenient for design of the mechanical structures.

The NIF amplifiers are suspended beneath a support frame in order to provide access from the bottom to replace slabs, flashlamps, and blast

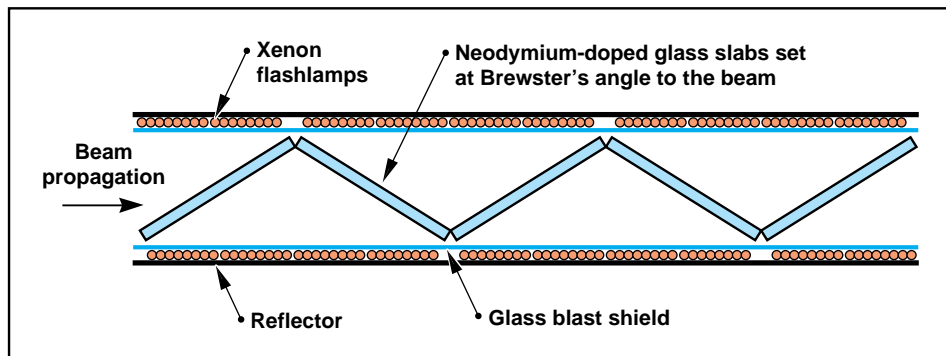


**Figure 4.** Top view of a large glass amplifier using slabs of neodymium-doped glass set at Brewster's angle to the beam and pumped by xenon flashlamps. The glass blast shields protect the slabs from acoustic disturbances and dirt generated by the flashlamps.

shields. It is extremely important to minimize contamination of the amplifiers by particles that otherwise might burn into the glass surfaces when illuminated by the intense flashlamp or laser light. Access from the bottom of the amplifiers ensures that service personnel and equipment are always below and downwind from sensitive surfaces, so that dirt falls to the floor and not into open amplifier structures. Figure 6 shows a servicing cart in the process of installing a stack of four laser slabs into the amplifier structure.

The pulsed-power system for the NIF uses advanced self-healing energy storage capacitors developed for use in Strategic Defense Initiative projects. These capacitors store energy at about four times the density and half the cost per joule of conventional capacitors, such as those used in the Nova laser facility at LLNL.

The number of amplifier slabs and their distribution among the three amplifiers were chosen to maximize the output power of the laser over the desired range of pulse shapes. For short pulses, the limit is set by nonlinear effects in amplifiers 2 and 3. For long pulses, the limit switches over to nonlinear effects in amplifier 1 and the limit set by the total amount of energy stored in the slabs. We might have eliminated amplifier 3 and placed 9 or 11 slabs in the amplifier 2 position. However, the polarizer coating suffers optical damage at a rather low fluence (energy per unit area). Such damage limits the laser output fluence to significantly less than we can run with the configuration shown in Figure 3. Notice that amplifier blocks are restricted to have an odd number of slabs (see Figure 4) so that gain gradients in the end slabs cancel.

### Spatial Filter

The NIF has two spatial filters in each beamline. In essence, a spatial

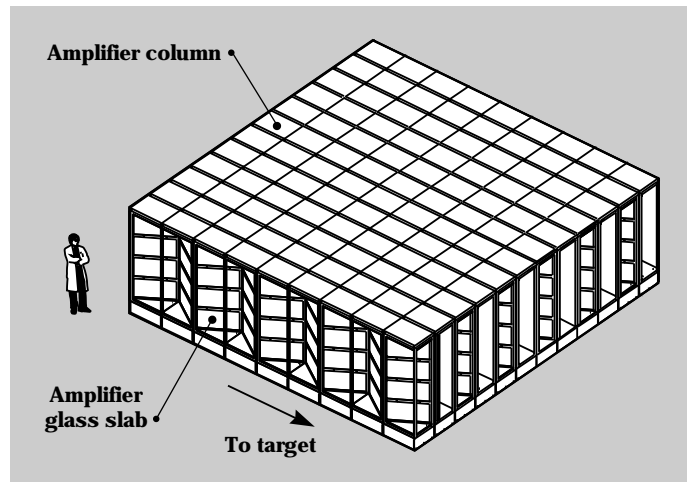


**Figure 5.** The main cavity amplifier assembly is typical of all the NIF amplifiers. Notice that a column consists of an amplifier that is 4 beams high. Groups of columns that are 12 beams wide form an amplifier assembly.

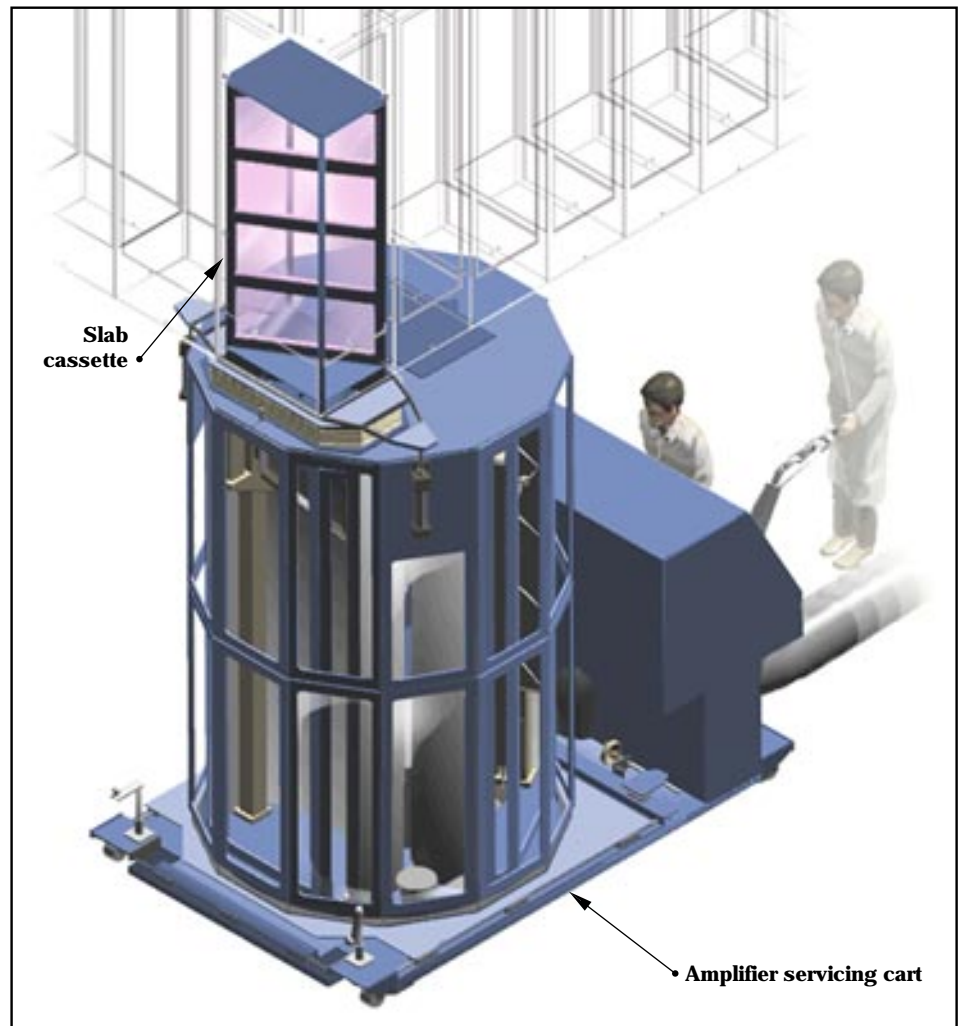


**Figure 6.** To facilitate maintenance, the slab and flashlamp cassettes shown at the top will be changed from underneath an amplifier column using a special cart. This approach will allow the critical amplifier components to be protected from the laser bay environment at all times.

filter—or image relay pair—is a pair of lenses separated by the sum of their focal lengths. A parallel beam incident on one lens comes to a focus in the center and emerges as a parallel beam at the other lens.

Spatial filters serve several functions in large lasers. For NIF, we positioned a pair of lenses so that an image of the very clean intensity profile injected from the preamplifier reforms near the amplifiers and at the frequency converter. Diffraction causes intensity noise to grow in laser systems, but this growth is reset to zero in the vicinity of an image of the original input profile. In addition, nonlinear effects in the laser cause small-scale intensity noise in the laser to grow, but this

small-scale noise comes to a focus displaced to the side of the main focus in the spatial filter. This displaced focus means that we can place a small pinhole at the focal plane that blocks this noise while allowing the main beam to go through. In addition, the focal plane inside the spatial filter gives us a convenient location for injecting the input pulse from the preamplifier without requiring any additional, expensive, large-aperture optical components.

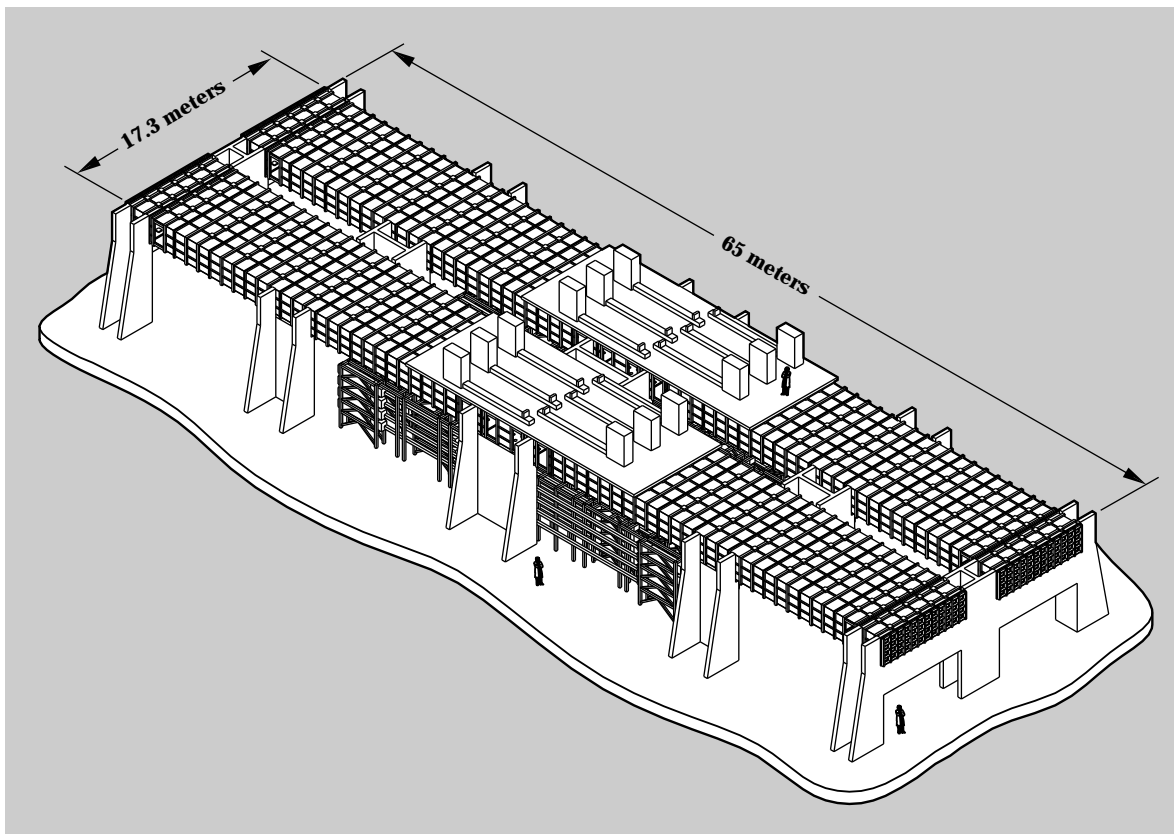
Because the intensity near the focal plane is very high, the spatial filters in large lasers such as NIF must be operated in a vacuum. **Figure 7** shows the large transport spatial filter vacuum vessel for NIF. The cavity spatial filter is similar, but somewhat shorter.

### Pockels Cell and Polarizer

A Pockels cell uses electrically induced changes in the refractive index of an electro-optic crystal, such as KDP (potassium dihydrogen phosphate or  $\text{KH}_2\text{PO}_4$ ) to rotate the polarization of light. When combined with a polarizer, the Pockels cell can serve as an optical switch that directs light into one or the other of two possible paths, and it is used for this function in the NIF laser.

Conventional Pockels cells require a crystal that is roughly the same thickness as the beam diameter. A crystal this thick is completely impractical for the NIF's 40-cm beam. Instead, the Pockels cell used in the NIF laser is a new type developed at LLNL. As shown in **Figure 8a**, it contains a thin plate of KDP placed

**Figure 7. Spatial filters in large lasers must contain a vacuum. Shown here is the transport spatial filter vacuum vessel for NIF. The basic functions of the transport spatial filter and cavity spatial filter are similar, but their lengths and internal components are different. Each vessel contains 48 beams. The entire structure is supported from the floor by reinforced concrete pillars. The pulse-generation system is located below the center section. Laser diagnostic units are supported by a frame attached to the filter top. Access to internal mechanisms is via doors on the vessel sides.**



between two gas-discharge plasmas. The plasmas serve as conducting electrodes, which allow us to charge the surface of the thin crystal plate electrically, but they are so tenuous that they have no effect on the high-power laser beam passing through the cell. **Figure 8b** shows a plasma electrode Pockels cell of this sort with a clear aperture of 35 cm. The device is now operating in our Beamlet Demonstration Project at the full laser fluence proposed for the NIF.

The polarizer for the switch is a multilayer dielectric coating set at Brewster's angle to the beam. These

thin-film polarizers are difficult to manufacture, but research supported by LLNL at commercial manufacturers has improved their process control and demonstrates that large polarizers meeting the NIF specifications are now available.

### Deformable Mirror

The NIF laser must have beam quality high enough that it can place all of the energy from each beamlet into a circle of about half a millimeter in diameter at the center of the target chamber. It is possible to purchase optical components finished well enough to achieve this goal, but the

cost of fabrication is higher than we would like.

We can use less expensive components if we design the laser to include an adaptive correction system that compensates for distortions in the beam. An adaptive system also allows us to compensate for other important distortions, such as thermal gradients. Recent advances in adaptive optics in the Atomic Vapor Laser Isotope Separation program at LLNL, and at several commercial companies and government research facilities, show that the cost of the deformable mirror, sensor, and processor technology required to

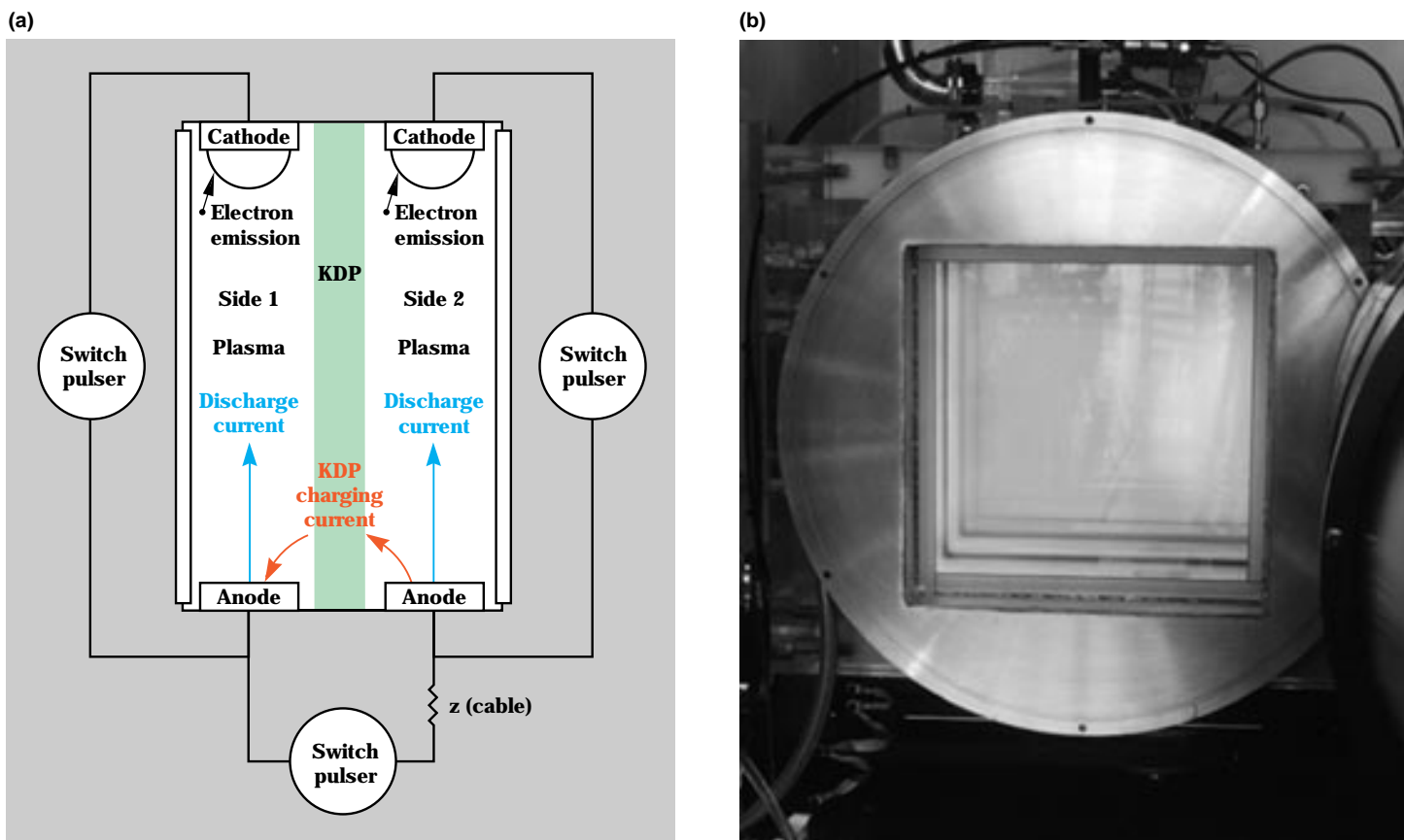


**Figure 8.** (a) The Pockels cell optical switch. This optical switch uses plasma as transparent, high-damage-threshold electrodes to charge the potassium dihydrogen phosphate (KDP) crystal. (b) A large-aperture, plasma electrode Pockels cell installed in the Beamlet Demonstration Project. Tests show that this device meets the requirements for timing, efficiency, and stability needed for NIF.

implement such a system has fallen to the point that adaptive correction systems are very desirable for the NIF facility. **Figure 9** shows a typical deformable mirror that uses electrostrictive actuators to bend the mirror surface to compensate for wavefront error. This mirror is installed on the Beamlet Demonstration Project, where we are studying its performance. The NIF will use a similar, but larger, mirror as **mirror LM1** in **Figure 3**.

**Frequency Converter**

A neodymium glass laser generates light at a wavelength of about 1 micrometer in the infrared region. However, we know that inertial

fusion targets perform much better when they are driven with ultraviolet radiation. The NIF laser will convert the infrared (1.05- $\mu\text{m}$ ) light to ultraviolet (approximately 0.35  $\mu\text{m}$ ) using a system of two nonlinear crystal plates made of KDP, the same type of crystal that is used in the Pockels cell.

**Figure 10** shows the arrangement of the two crystal plates. The first plate converts two-thirds of the incident 1.05- $\mu\text{m}$  radiation to the second harmonic at 0.53  $\mu\text{m}$ . Then the second crystal mixes that radiation with the remaining 1.05- $\mu\text{m}$  light to produce radiation at 0.35  $\mu\text{m}$ . This process has a peak efficiency greater than 80%, and the

efficiency can exceed 60% for the complex pulse shapes used to drive ignition targets.

**Target Area and Target Diagnostics**

**Figure 11** shows an end view of the NIF target area. From this perspective, we can see the beam paths from the laser output through the turning mirror array to the target chamber. The target chamber is a 10-m-diameter aluminum sphere. The beams enter the chamber in two conical arrays from the top and two from the bottom through final optics packages mounted to the target chamber. **Figure 12** shows a final

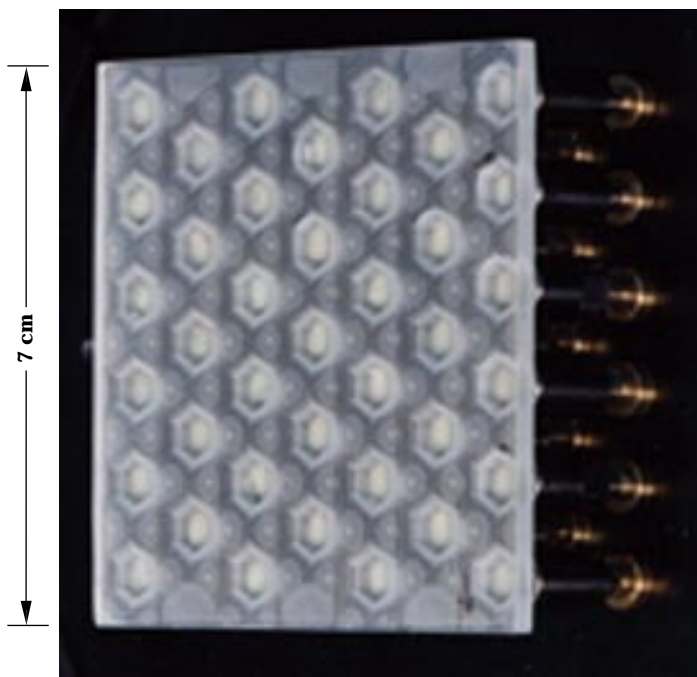


**Figure 9.** The cavity mirror farthest from the target area (**LM1** in **Figure 3**) is a deformable mirror used for performing wavefront corrections of the beam. Electrostrictive actuators bend the mirror surface to compensate for wavefront error. This photograph shows a 70- $\times$  70-mm deformable mirror currently used on the Beamlet Demonstration Project. The NIF will use a mirror that is similar to this one, but larger.

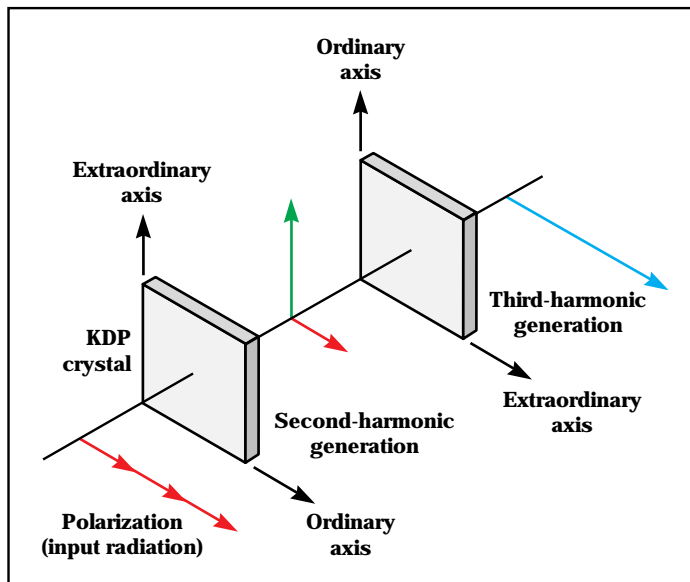


**Figure 10.** The NIF configuration for frequency conversion to the third harmonic using two KDP crystal plates. The NIF laser generates light in the infrared region (this 1.05- $\mu\text{m}$  wavelength light is shown as red in the drawing). However, inertial fusion targets perform better with ultraviolet radiation. This 0.35- $\mu\text{m}$  wavelength light is called the third harmonic (shown as blue). The first KDP crystal (left) converts two-thirds of the input radiation (red) to second-harmonic radiation (green). The second crystal mixes the remaining input radiation with the second harmonic to produce third-harmonic radiation (blue). Peak conversion efficiencies can exceed 80%.

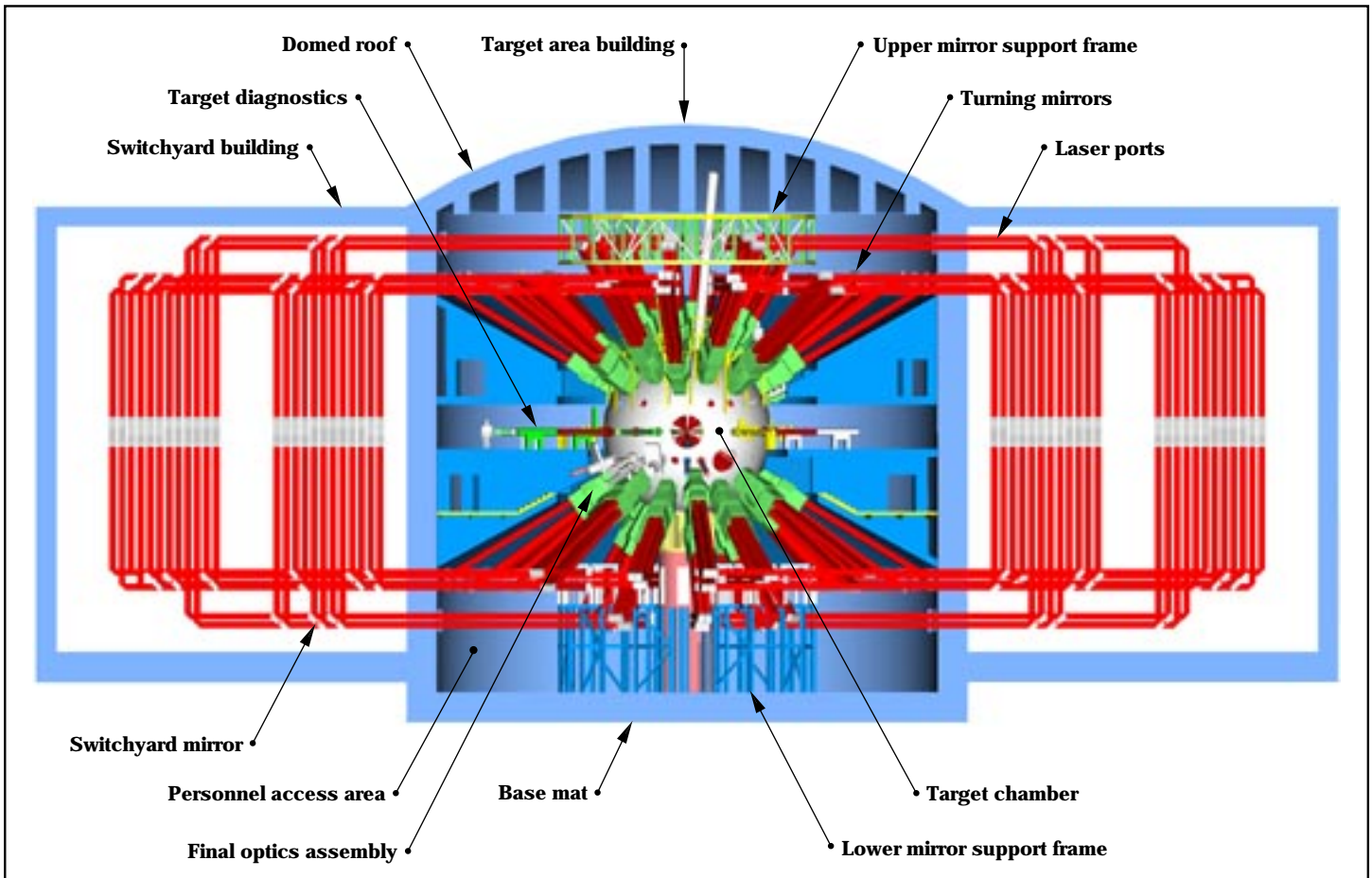
optics assembly subsystem. Diagnostic instruments, such as x-ray spectrometers, microscopes, and cameras, are mounted around the equator and at the poles of the target chamber.

Figure 13a is a scale drawing of a typical fusion ignition target that will be used with this chamber. The target is a metal cylinder—typically made of gold or lead—about 6 mm in diameter and 10 mm long. It contains a plastic fusion capsule about 3 mm in diameter. The capsule is chilled to a few degrees above absolute zero

and is lined with a layer of solid deuterium–tritium (DT) fusion fuel. The hollow interior contains a small amount of DT gas.

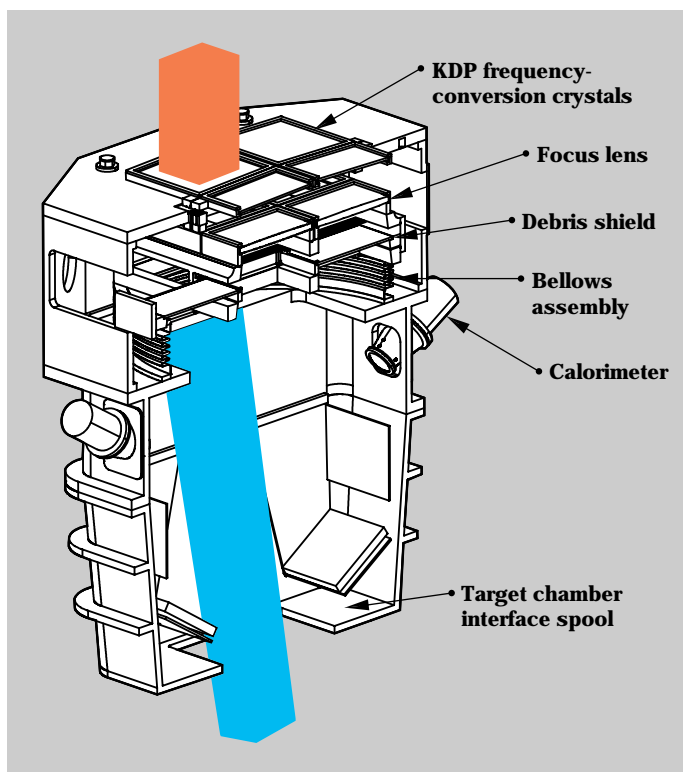
Figure 13b is an artist's 3-D rendering showing how laser beams deposit their energy on the inside surface of the metal cylinder or "hohlraum" where the energy is converted to thermal x rays. The x rays heat and ablate the plastic surface of the ignition capsule, causing a rocket-like pressure on the capsule and forcing it to implode.

Figure 14 is an x-ray image of a target shot from the Nova laser showing the glowing spots where Nova's ten beams strike the inside surface. In this image, artists drew in the laser beams and the outline of the cylinder, which are invisible in an x-ray photograph. For this experiment, the metal wall was made thin enough that some of the x rays leaked through to be photographed. Thicker walls are used for most targets. In the language of fusion research, this target is called an "indirect-drive" target because the



**Figure 11.** Cut-away view of the NIF target area showing the major subsystems. The laser beams focus energy onto a target located at the center of the target chamber, which is housed in a reinforced-concrete building. Target diagnostics mounted on the chamber will collect the experimental data.

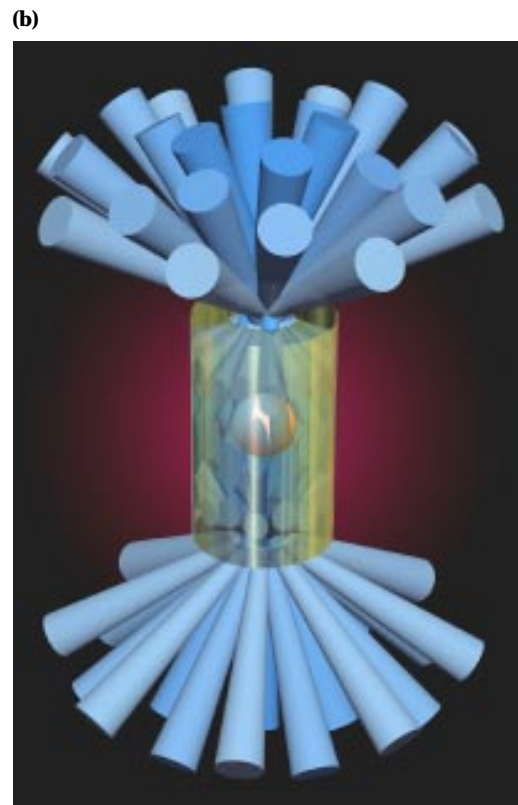
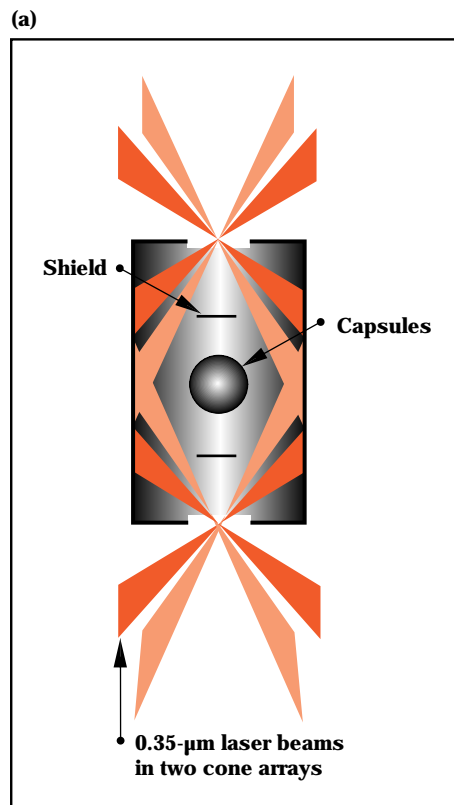
**Figure 12.** The final optics assembly is a single, integrated structure that is mechanically supported by and fastened to the target chamber. The frequency-conversion crystals (see **Figure 10**) are shown at the top. This system will convert four infrared beams to the third harmonic, focus the beams onto a target, and provide beam smoothing and color separation. The calorimeter is used to obtain energy measurements on the incident beam.



laser beams do not strike the fusion capsule directly. NIF can also study “direct-drive” targets in which there is no hohlraum and the beams do strike the capsule directly.

To illustrate the type of diagnostics we use to study fusion targets, **Figure 15** shows a sequence of pictures of a fusion capsule implosion from a direct-drive target on the Omega laser at the University of Rochester. Here, the fusion capsule is similar to, but smaller than, the one shown in **Figure 14**. (Indirect-drive targets give similar pictures, but the hohlraum and other complications make the pictures less clear.) The images are from an x-ray framing camera microscope (that is, the sequence of frames was taken by a very-high-speed motion picture camera). Each frame lasts for 50 picoseconds (50 trillionths of a second).

**Figure 13.** (a) Scale drawing of a typical fusion target. The outer metal cylinder, usually made of either gold or lead, is about 6 mm in diameter. Inside is a plastic fusion capsule that is about 3 mm in diameter. The capsule is lined with a layer of solid deuterium-tritium (DT) fusion fuel, and the hollow interior contains a small amount of DT gas. Laser beams enter the target in two conical arrays. The outer and inner cones are shown at the top and bottom of the target. (b) An artist’s 3-D rendering of the laser beams depositing their energy on the inside surface of the hohlraum where they are converted to x rays that heat the target internally, causing it to implode and ignite.



In **Figure 15a**, the 0.25-mm-diameter capsule lights up brightly as the laser beams first strike its cold surface. In the next several frames, the surface of the capsule blows outward, and the gas fill is accelerated towards the center, compressing to a very high density. In **Figure 15g**, the gas begins to collide with other imploding gas at the center of the capsule and comes to a stop. As it stops (or stagnates), the temperature shoots up to a value at which fusion reactions can begin. The high-temperature region at stagnation can be seen as a bright x-ray spot in **Figures 15g through 15j**. If this were an ignition target shot using the NIF, the hot gas core or “spark plug” would ignite the surrounding, relatively cold DT layer, producing roughly 10 megajoules of fusion yield. The hot target plasma then expands and cools in **Figures 15k and 15l**.

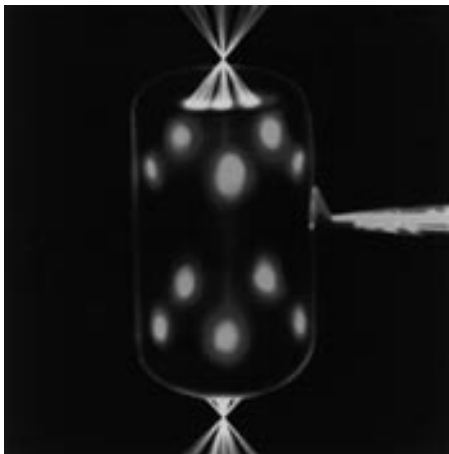


**Figure 14.** X-ray image of a target shot from the Nova laser. The glowing spots are where Nova’s ten beams strike the inside surface of the target’s thin, cylindrical metal wall. This target is called “indirect drive” because the laser beams do not directly strike the inner spherical capsule, which contains DT fuel. The outer shell and beam paths, invisible in an x-ray photograph, are drawn by an artist to show where they were located in the original target.

Ten megajoules is not an enormous amount of energy. It roughly corresponds to the heat released in burning an 11-ounce water glass full of gasoline (about 312 cm<sup>3</sup>). However, the energy in a fusion target is produced and radiated away in less than a nanosecond from a volume with a diameter of only about a fifth of a millimeter. To do that, the target material must reach conditions that are found in nature only deep within stars and other hot celestial objects or deep within nuclear weapons.

In **Figure 15**, the drive on the target was deliberately distorted, so the implosion formed a little to the right of center from the camera’s point of view. A perfectly centered implosion gives higher temperatures

and better target performance. Nevertheless, these pictures are good illustrations of how target experimenters study the effects of nonideal conditions, such as nonuniform drive pressure, and compare test results to their theoretical models.

### NIF Beamlet Demonstration Project

Glass lasers are a popular and well-known technology, but the NIF laser design is significantly different in many ways from existing large glass lasers (see the **box on p. 18**). To be quite sure that the NIF system will function as we project, it is prudent to test some of the differences well in advance of construction. In 1992, we

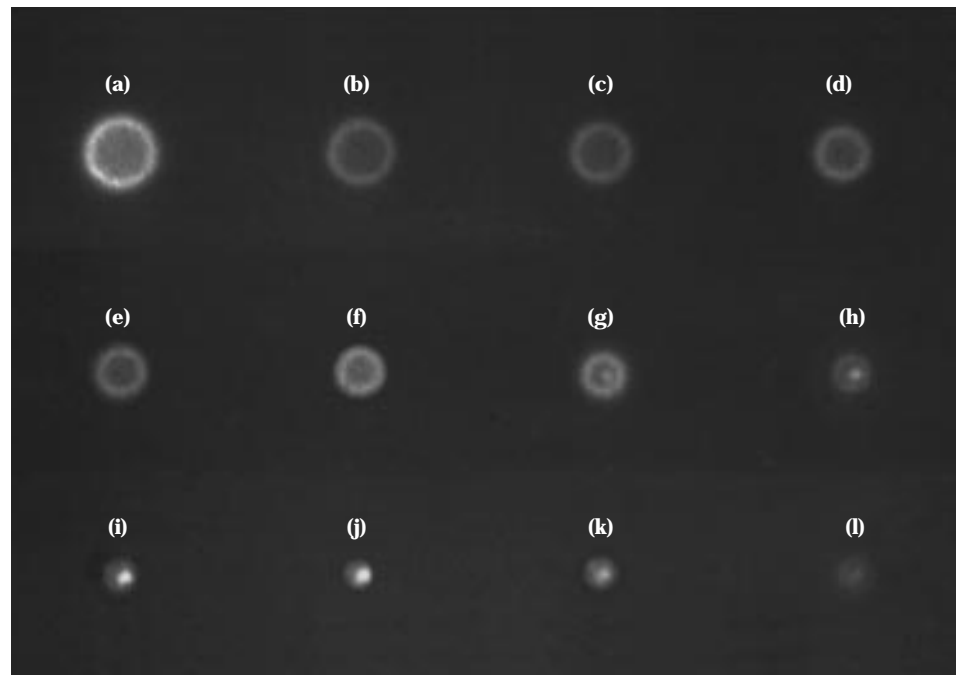


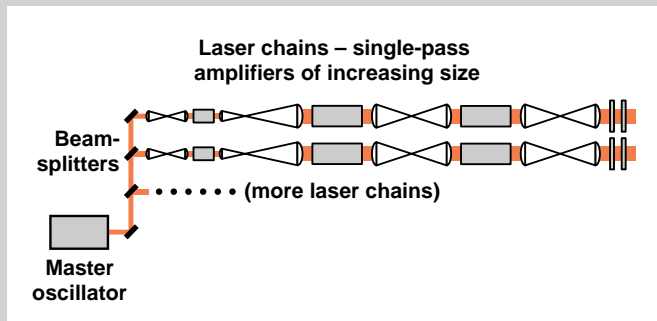
**Figure 15.** Sequence of pictures of fusion-target implosion taken with an x-ray framing camera microscope. Each frame lasts for 50 ps and is a positive image, so bright areas are regions of bright x-ray emission. (a) Laser beams strike the 0.25-mm-diameter cold target shell and start the implosion. (b) through (g) The outer surface of the shell blows off, and the inner part of the shell and gas implode. In (g), the gas fill collides with itself near the center of the implosion, and the rapidly increasing temperature produces a bright spot of x-ray emission. The central hot spot develops through (j) and then begins to expand and cool in (k) and (l).

## How the NIF Differs from Other Glass Lasers

The neodymium glass laser, invented in 1961, was one of the first types of laser to be developed. Researchers quickly realized that it could be scaled up to large beam apertures and extreme peak power. Many laboratories soon began developing glass laser hardware for research on nuclear fusion and other high-energy-density physics.

To reach high energy and power, large glass amplifiers are required. However, it is difficult and inefficient to generate a high-quality output beam from large amplifiers. The design that evolved was called the single-pass master-oscillator/power-amplifier (MOPA) chain.

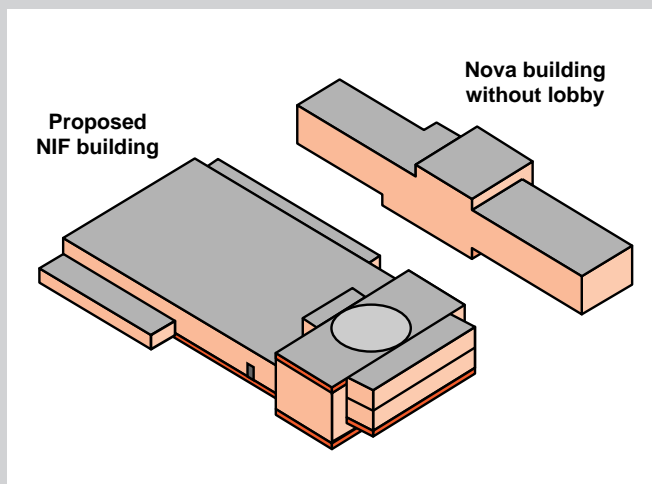
As shown in the illustration below, a MOPA design uses a small oscillator to produce a pulse of a few millijoules with a beam diameter of a few millimeters. After passing through other components, such as a preamplifier, the pulse is divided and makes a single pass through a chain of amplifiers of gradually increasing size. The amplifiers are separate components rather than being grouped in large arrays, as in the NIF design.



The MOPA is a low-risk, but expensive, approach to constructing large glass lasers. Limitations include considerable setup time and cost; very long propagation paths; the need for critical alignments and physical changes to many different components; and the fabrication, assembly, and maintenance of a large number of parts.

The Nova laser at LLNL is the largest operating glass MOPA fusion laser. It contains five sizes of amplifiers with a total of 41 slabs of glass in each of ten laser chains. Compared to the size of the Nova facility, the compact design of the NIF multipass

system allows us to put a laser with a typical output that is 40 times larger than Nova's into a building only about twice the size (although the Nova laser does not completely fill the building).



For truly large lasers, such as NIF, the MOPA design has another important disadvantage. The NIF fusion-ignition targets require pulses with a length of 3 to 5 ns. At this pulse duration, we can extract most of the energy stored in the laser glass. When we do, the tail end of a pulse has a much lower gain than the front end, a difference we call saturation pulse distortion (SPD). MOPA designs require larger and more expensive amplifiers and preamplifiers under these conditions. Multipass lasers, such as NIF, solve the problem of SPD without the need for larger preamplifiers. In contrast, Nova uses much shorter pulses and does not extract as much of the stored energy.

Even when the Nova laser was designed in 1978, we knew that a multipass design would be potentially much less expensive to build. However, the necessary component development that was still required meant additional risks and possible delays. The NIF laser design is a result of development efforts started many years ago for components such as advanced oscillators, amplifiers, and Pockels cells. Today, our Beamlet Demonstration Project integrates all of these new developments. This effort is showing that the technology has now progressed to the point that a large, multipass glass laser can be built with low risk.

established the Beamlet Demonstration Project (or the Beamlet for short) to test some of the new features. The Beamlet has now been completed and is currently operating reliably up through the frequency converters at fluence and intensity levels projected for NIF.

We built a single prototype rather than a large array of beams because it was clearly much too expensive to construct a full NIF beamline with  $4 \times 12$  amplifier blocks and multiple beamlets. We did, however, build the main laser amplifiers as an array stacked two high and two wide because it was important to begin to

understand the engineering of large amplifier arrays. To reduce costs, only one of the four apertures in the array contains high-quality laser glass. The other three apertures contain an inexpensive glass that absorbs flashlamp light in a way that resembles the laser glass. In addition, the amplifiers and other laser hardware rest on the floor rather than hanging from a support frame as they will in the NIF design. Components resting on the floor were more convenient for the room we had available, although the system is more difficult to keep clean than that in the NIF design.

The NIF laser design has evolved over the past two years as we try to optimize its cost and match its performance to the wide range of possible experiments that might be conducted. This evolution has led to a few other small differences between the Beamlet and the NIF design presented in the Conceptual Design Report and discussed in the first part of this article. For example, the beam apertures for the Beamlet are slightly smaller than those for NIF, and the laser is shorter. We used 16 rather than 19 slabs of glass, and these slabs are distributed in a ratio of 11-0-5 (eliminating amplifier 2) rather than

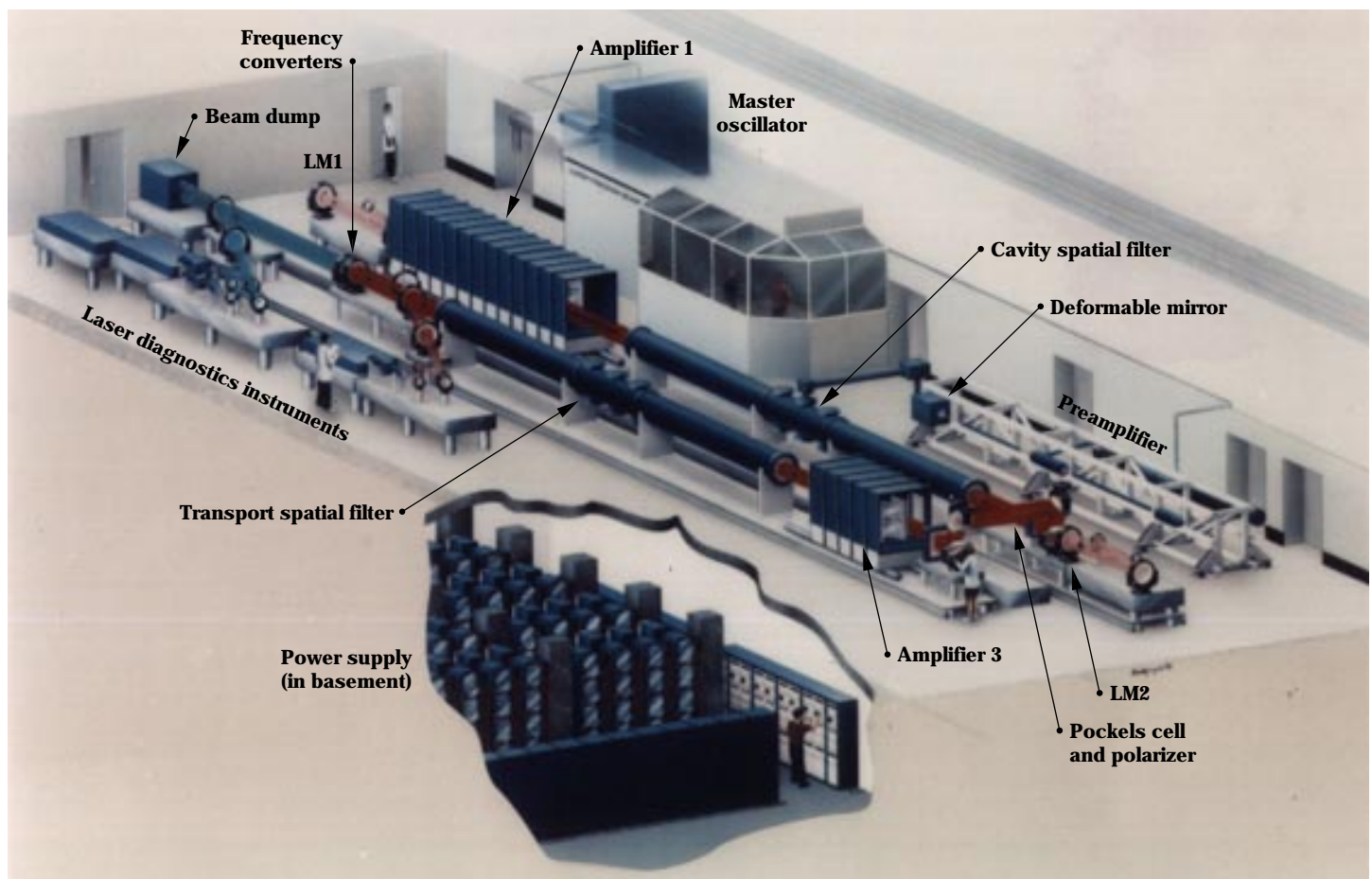


**Figure 16.** The Beamlet is a scientific prototype of the NIF multipass laser. This demonstration unit, which is now operating at LLNL, uses essentially the same technology as that for NIF but with one output channel rather than 192.

9-5-5 in the **three amplifiers shown in Figure 4**. The NIF distribution gives better performance for pulses of 4 to 5 ns and longer, whereas the Beamlet distribution is better for short pulses. The input pulse from the preamplifier is injected into the cavity spatial filter rather than the transport spatial filter. This design makes the front end slightly larger because the pulse does not see the small-signal gain of amplifiers 2 and 3. However, the design simplifies alignment if the input pulse is used for laser alignment, as it is in Beamlet (but not NIF). Otherwise, the Beamlet has all the NIF components and features shown in **Figure 4**.

**Figure 16** is a drawing of the Beamlet facility. The master oscillator and preamplifier are the same technology as that for NIF, but with only one output channel rather than 192. The laser pulse reflects from a deformable mirror (see **Figure 9**) and enters the cavity transport spatial filter. We use a deformable mirror in this position rather than in the LM1 position described for NIF because this smaller mirror could be adapted from an existing design at very low cost. The pulse then passes through amplifier 1 and reflects from mirror

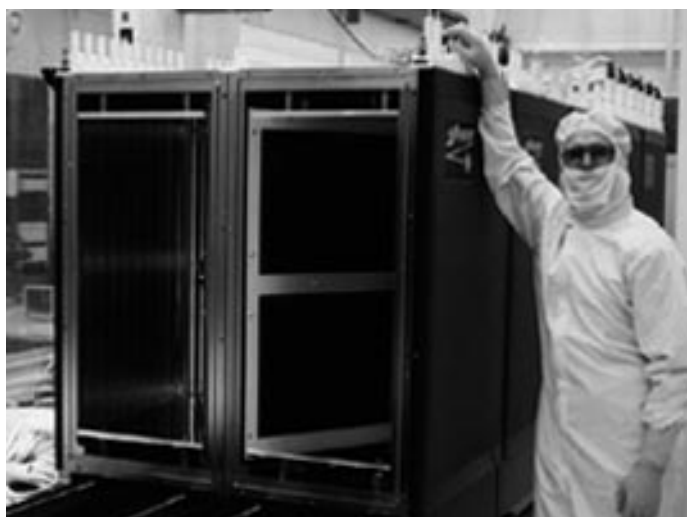
LM1, returns through the amplifier and cavity spatial filter to the Pockels cell and LM2, makes a second round trip through amplifier 1, and returns through the Pockels cell to reflect from the polarizer, just as described for NIF.

The output pulse then reflects from three turning mirrors that are used to fold the Beamlet optical path in two so that it fits in the available space. The pulse passes through amplifier 3 and the transport spatial filter, then enters the frequency-conversion crystals. Beam splitters direct samples of the infrared and ultraviolet beams to diagnostic instruments located near the frequency converters. Most of the beam energy is absorbed by an absorbing glass beam dump at the end of the beamline.

**Figure 17** is a photograph of the Beamlet amplifier. The amplifier's clear aperture is 39 cm, or essentially the same as the 40-cm aperture proposed for NIF. The amplifiers perform exactly as predicted from design codes (elaborate computer simulations) we developed for smaller amplifiers.

Large amplifier apertures such as this lead to a less expensive NIF because there are fewer beamlets,

**Figure 17.** The 2 × 2 amplifier module for Beamlet shown during assembly. To reduce costs, only one of the four apertures in this array contains high-quality laser glass. The clear aperture of 39 cm is essentially the same as that proposed for NIF. Such large amplifier apertures lead to a less expensive NIF.



and many of the costs of a system scale with the number of beamlets rather than their size. However, amplified spontaneous emission causes the gain of large amplifiers to drop by a few percent at the edges of the aperture. We compensate for this gain drop on Beamlet (and NIF) by making the input pulse more intense around the edges.

The large plasma-electrode Pockels cell switch installed on Beamlet is shown in **Figure 8b**. Only about 30 J leak through the polarizer when we set this switch to reflect 6 kJ from the polarizer, so the Pockels cell and polarizer are remarkably efficient.

**Figure 18** shows the infrared output energy from Beamlet as a function of the input energy from the preamplifier. For this set of shots, we set the beam aperture to 34 × 34 cm, a value limited by the 35-cm clear aperture of the Pockels cell crystal. The output energy matches the theoretical model (solid line) very well. We have fired the system at an output up to 13.9 kJ at

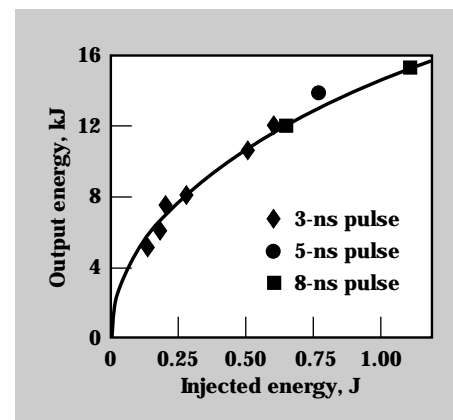


**Figure 18.** Performance of the Beamlet amplifier for a 34- × 34-cm beam at three different pulse lengths. The infrared output energy is plotted as a function of the input or injected energy from the preamplifier. This plot shows that the output energy matches our theoretical model (solid line) quite well.

5 ns and at somewhat higher output for longer pulses. At 5 ns, the fluence (energy per unit area) across the flat-top part of the beam is  $14.3 \text{ J/cm}^2$ . This is about 7% above the nominal operating point for the NIF ignition target in the Conceptual Design Report.

We recently conducted the first series of Beamlet frequency-conversion tests. For these tests, the aperture of the frequency-conversion crystals limited the beam aperture to  $29.6 \times 29.6 \text{ cm}$ . We have operated the conversion crystals up to  $8.7 \text{ J/cm}^2$  ultraviolet output in 3-ns pulses, which is once again about 10% above the NIF nominal operating point. The conversion efficiency from infrared to ultraviolet was just over 80% for square pulses, as anticipated. The maximum ultraviolet energy demonstrated to date is 6.7 kJ. It is

likely that we can operate at somewhat higher fluences, but we will not push beyond the nominal NIF fluences and run the risk of damaging optical components until we have conducted all of the most critical tests on the system. We will certainly have higher energies when we obtain larger crystals and expand the beam size later this year. We will not quite reach the nominal NIF beam aperture of  $36 \times 38 \text{ cm}$  because the Beamlet components are smaller and the beam path is shorter than for NIF. Nevertheless, we should be able to run experiments at apertures of about 34 to 35 cm. We have also run complex shaped pulses of the sort required for ignition targets. In these experiments, we obtained conversion efficiency up to 65% and fluence and energy similar to those for square pulses.

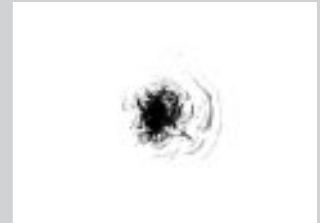
It is important to have very uniform intensity profiles in a fusion laser. Uniform profiles minimize the risk of damage caused by intensity maxima in the beam and help to maintain high frequency-conversion efficiency. Figure 19 shows intensity profiles of the infrared and ultraviolet beams from Beamlet as recorded by television cameras in the laser diagnostics area. The beam profiles are very smooth and flat across the center, as desired, and they roll off smoothly to zero intensity in a small margin around the edge.

Low phase distortions on the beam are also important. Phase distortions not only prevent the beam from focusing on a small spot, but they also degrade the process of frequency conversion. Figure 20 shows the distribution of Beamlet energy at the focus of a lens (in the far field).

## Laser Damage in Optical Materials

When a laser beam strikes a component, it can cause optical-induced damage. The damage usually appears only at high fluence (energy per unit area) and is caused by a small flaw or contamination by foreign material. Flaws or contaminants can absorb enough energy to melt or vaporize and then disrupt the surrounding optical material. The cost of a large laser is roughly proportional to the total beam area, so we push laser designs to the highest fluence that can be tolerated without damage to minimize the beam area and cost.

On the left is a view through a microscope of a tiny light-absorbing defect in a piece of optical glass. This particular defect is about a twentieth of a millimeter in diameter, or about the diameter of a human hair, and it is 10 or 20 times larger than the typical defect that concerns us. When an intense laser beam strikes the defect, its surface evaporates and explodes causing tiny cracks in the glass. As shown on the right, the cracks tend to grow larger with each laser shot, and the damaged spot eventually gets large enough to disrupt the laser beam quality seriously.



In the past 15 years, the number of defects that initiate laser damage in optical materials has decreased dramatically. The decrease is a result of painstaking research at commercial suppliers and various research laboratories. Much of the work was funded by the LLNL laser program and other programs interested in constructing large lasers. As a result, the NIF laser will operate at fluence levels that would have been unthinkable at the time Nova was constructed. As one example, the average ultraviolet fluence at the output of our Beamlet Demonstration Project is more than three times the average fluence that would have been safe for the optical components that were available when Nova was built.

These data reveal that about 95% of the energy is within an angle of  $\pm 25$  microradians from the center of the spot. Because the NIF requirement for ignition targets is  $\pm 35$  microradians, this spot meets that requirement. Nevertheless, we would like to improve this value even more because some potential experiments could use a smaller spot.

We obtained the far-field spot in [Figure 20](#) at the end of a sequence that included four full-power Beamlet shots over about 10 hours. Much of the remaining structure in the spot

(smaller peaks on the curve) is caused by gas turbulence in the amplifiers and beam tubes. Beamlet’s deformable mirror, which was in operation during this test, can correct the long-term thermal distortions in the amplifier slabs very effectively. Indeed, this spot is smaller—by a factor of four or five—than it would be without such correction. However, the deformable mirror system cannot respond rapidly enough to correct for gas turbulence. When the glass amplifier slabs are cold and the temperature is uniform, the deformable mirror has less effect

on the spot size, and the spot size is also somewhat smaller than that shown in [Figure 20](#). We have only begun to study the performance of the deformable mirror, but even these early results confirm that adaptive optics will be a highly valuable addition to NIF.

### Next Steps Toward NIF

Our Beamlet tests to date demonstrate clearly that large, multipass laser systems can operate at the nominal operating conditions proposed for the NIF. We will now proceed to explore more extreme operating conditions and to demonstrate that the proposed target optics will give spots of the desired size and uniformity at the plane of the target in the far field. We will also test many other features suggested for NIF, such as new glass compositions, changes in amplifier pumping conditions, and alternate switch technology. The results from our Beamlet Demonstration Project, along with the models and design codes we are testing, will ensure that we can have great confidence in the performance projected for NIF.

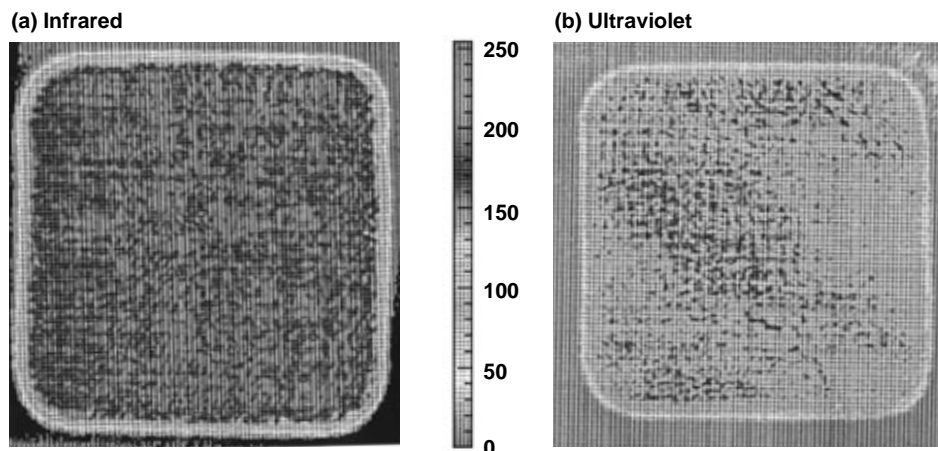
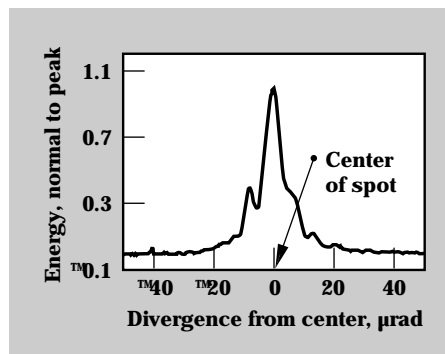


**Figure 19.** A fusion laser must have uniform intensity profiles. These intensity profiles obtained from Beamlet are smooth and flat across the center during frequency conversion from (a) infrared to (b) ultraviolet light. The small margins indicate that the profiles roll off smoothly to zero intensity around the edges of the 30- x 30-cm beam.

**Figure 20.** The distribution of Beamlet energy at the focus of a lens (in the far field). This curve shows that about 95% of the energy is within  $\pm 25$  microradians of the center of the spot, well within the design requirements for NIF ignition targets.



**Key Words:** adaptive optics; Beamlet Demonstration Project; deuterium–tritium (DT) fuel; fusion energy; multipass lasers; National Ignition Facility (NIF); neodymium glass lasers; Pockels cell; potassium dihydrogen phosphate (KDP).



*For further information contact  
John R. Murray  
(510) 422-6152.*